Mechanism of Spontaneous DNA−DNA Interaction of Homologous Linear Duplexes†

Anna A. Neschastnova,‡ Victoria K. Markina,‡ Vladimir I. Popenko,§ Olesya A. Danilova,‡ Roman A. Sidorov,‡ Gennady A. Belitsky,‡ and Marianna G. Yakubovskaya*,‡

Institute of Carcinogenesis, Blokhin Cancer Research Center RAMS, Kashirskoye shosse 24, Moscow 115478, Russia, and Engelgardt Institute of Molecular Biology, Russian Academy of Sciences, ul. Vavilova 32, Moscow 117984, Russia

Received November 19, 2001; Revised Manuscript Received February 12, 2002

ABSTRACT: Previously, we demonstrated the interaction of homologous linear duplexes with formation of four-way DNA structures on the model of five PCR products. We propose that homologous duplex interaction is initiated by the nucleation of several dissociated base pairs of the complementary ends of two fragments with Holliday junction formation, in which cross point migration occurs via spooling of DNA strands from one duplex to the other one, finally resulting in complete resolution into new or previously existing duplexes. To confirm that DNA−DNA interaction involves formation of four-way DNA structures with strand exchange at the cross point, we have demonstrated the strand exchange process between identical duplexes using homologous fragments, harboring either biotin label or ^{32}P-label. Incubation of the mixture resulted in the addition of ^{32}P-label to biotin-labeled fragments, and the intensity of ^{32}P-labeling of biotinylated fragments was dependent upon the incubation duration. DNA−DNA interaction is not based on surface-dependent denaturing, as Triton X-100 does not decrease the formation of complexes between DNA duplexes. The equilibrium concentration of Holliday junctions depends on the sequences of the fragment ends and the incubation temperature. The free energy of Holliday junction formation by the fragments with GC and AT ends differed by 0.6 kcal/mol. Electron microscopic analysis demonstrated that the majority of Holliday junctions harbor the cross point within a 300 base pair region of the fragment ends. This insight into the mechanism of homologous duplex interaction extends our understanding of different DNA rearrangements. Understanding of DNA−DNA interaction is of practical use for better interpretation and optimization of PCR-based analyses.

The phenomenon of DNA−DNA interaction of homologous linear duplexes has been shown on synthetic DNA duplexes (*1*), purified PCR products (*2*, *3*), and DNA fragments restricted from the genome of simian virus 40 and linearized plasmid (*4*−*6*). Standard thermodynamic parameters for DNA branching of synthetic duplexes at temperatures close to physiological values showed that the unfavorable enthalpy represents the loss of approximately two to three base pair interactions at the branched structure relative to the corresponding duplexes (*1*, *7*). Elucidation of the mechanism of homologous duplex interaction resulting in branched DNA structure formation is of practical and theoretical importance. In vivo four-stranded DNA structures (*8*), Holliday junctions (HJ),[1] arise transiently as intermediates in genetic recombination (*9*), and they can form at either the terminus or the origin of replication (*10*). This process is controlled by DNA conformation (*11*) and DNA−protein interaction (*12*); however, underlying mechanisms of DNA−DNA interactions may be also critical. Since the introduction of PCR-based methodologies, homologous DNA duplex solutions are widely used in both scientific and clinical investigations. Understanding of the processes of diverse DNA structure appearance in homologous duplex solutions should help to interpret the results and to optimize the analyses when using PCR products in nondenaturing conditions.

Previously, we revealed DNA−DNA interaction using gel electrophoresis of solutions of purified PCR products by appearance of the additional bands corresponding to double size DNA fragments (*3*). The efficiency of PCR product purification was demonstrated, and the double-stranded (ds) structure of DNA fragments interacting was confirmed using several consecutive purifications and S1 nuclease analysis. HJ formation was shown to depend on DNA concentration. Thermodynamic equilibrium between duplexes, HJs, and complex branched DNA structures was demonstrated. Further, electron microscopy analysis of DNA extracted by electroelution and filtration from agarose gel slices of additional bands showed a high portion of symmetrical four-way DNA structures. Electron microscopy of the DNA solution extracted from the band of ds PCR product demonstrated predominantly linear fragments. The symmetry of all χ-structures observed made us conclude that DNA−DNA interaction occurs via HJ formation. However, in the

† This research was supported by a CDA-NIS grant from the NCI to M.G.Y., ITSC 832, and RFFI grants 01-04-06103, 00-04-48579, and 02-04-49064.

* Corresponding author. Fax: 7 095 323 58 22. E-mail: myakubovskaya@crc.umos.ru.

‡ Blokhin Cancer Research Center RAMS.

§ Engelgardt Institute of Molecular Biology, RAS.

[1] Abbreviations: HJ, Holliday junction; ds, double stranded; ss, single stranded.

10.1021/bi015959t CCC: $22.00
Published on Web 05/24/2002

investigation of Gaillard and Strauss (*4*) analogous results of electron microscopy of solutions of homologous linear fragments containing CA repeats were interpreted as four-way DNA structures without strand exchange. Additional confirmations of strand exchange at the cross points were considered to be necessary. If the four-way DNA structures revealed in our previous investigation were really HJs, their resolution should lead to a strand exchange process between identical DNA duplexes. And vice versa, demonstration of the strand exchange process in solutions of homologous duplexes in nondenaturing conditions confirms strand crossing in the χ-structures observed. Consequently, demonstration of the strand exchange process in solution of homologous duplexes was one of the aims of the present study.

On the basis of our electron microscopy results and modern theories of DNA structure (*13*−*15*), duplex melting, and fraying (*16*−*18*) we formed the hypothesis of homologous duplex interaction (*3*). We proposed that at temperatures close to physiological values the constant process of dissociation−reassociation of the duplex ends occurs, and when complementary ends of two homologous fragments are dissociated, these two duplexes might interact analogously to the model elaborated by Panyutin and Hsieh to analyze branch migration (*19*). In their experiments interaction of two homologous duplexes was initiated by the annealing of two single-stranded (ss) tails of one duplex to corresponding complementary ss tails of the other duplex, and then branch migration led to complete strand exchange and formation of new duplexes. In our case of absolutely homologous linear fragments the rate of HJ formation by homologous dissociated ends is much lower, and the branch migration process (*20*−*22*) may happen in either direction: both new and previously existing duplexes may be formed after HJ resolving. A similar mechanism of DNA duplex rearrangements based on the nucleation of the ends of unpaired strands was elaborated by Belotserkovskii et al. (*23*−*25*) for the process of dissociation of double D-loop DNA hybrids. Recently, the process of duplex end melting and fraying was described (*16*−*18*), and it was shown that the free energy of end base pair dissociation and the melting temperature of duplex ends depend on their sequences (*16*). Consequently, we proposed that incubation temperature and duplex end sequences modulating the structure of the duplex ends should influence the equilibrium between HJs and duplexes.

The goal of the present study was to demonstrate the strand exchange process between identical DNA molecules and dependence of HJ equilibrium concentrations on the sequences of the fragment ends and on the temperature of incubation and, therefore, to support our hypothesis of the mechanism of homologous linear DNA duplex interaction.

MATERIALS AND METHODS

PCR Products. Amplification was carried out using *Taq* DNA polymerase (Biomaster, Moscow) in reactions performed with PTC-100 (MJ Research, Inc.) thermocyclers. For amplification of DNA fragments we used the primers and protocols as follows: for the 157 bp fragment of human Ki-ras oncogene, 5′-GTGACACGCTTCCCTGGATTG-3′ (sense) or biotin-GTGACACGCTTCCCTGGATTG-3′ (sense) and 5′-ATGTCAGTCTGAGTCAGGCCCTCT-3′ (antisense), 95 °C for 2 min, 27 cycles (95 °C, 1 min; 54 °C, 1 min; 72 °C, 1 min), 72 °C for 10 min, 4 °C; for the 1254 bp fragment of human p53 cDNA with GC ends, 5′-GCGCGCGACACCGTTCCCTGGATTGG-3′(sense) and 5′-CCGGCCGCAGTCTGAGTCAGGCCCTCT-3′(antisense), and with AT ends, 5′-ATATATAACACCGTTCCCTGGATTGG-3′(sense) and 5′-TTAATTACAGTCTGAGTCAGGCCCTCT-3′(antisense), 95 °C for 2 min,′ 30 cycles (95 °C, 1 min; 58 °C, 1 min; 72 °C, 1 min), 72 °C for 10 min, 4 °C. Plasmids with p53 cDNA and Ki-ras 1 exon fragment used as templates were kindly given by P. Chumakov and Z. Ronai.

Gel Electrophoresis (Nondenaturing). Agarose (2% and 1.5%) (high resolution, Sigma) gels were run at 10 °C and 60 V in standard 0.089 M Tris−borate buffer, pH 7.5, containing 0.002 M EDTA. DNA was visualized by ethidium bromide staining.

DNA Purification from Agarose Gels Using the DNA-Binding Silica Matrix. The gel slice with the double-stranded PCR product was excised from the agarose gel after electrophoresis and purified using the DNA-binding silica matrix. After incubation in an equal volume of 6 M NaI at 55 °C for 30 min, the appropriate amount of silica matrix was added. The mixture was incubated at 24 °C for 30 min and centrifuged (2000*g* for 2 min), the pellet was washed twice with washing buffer [50 mM NaCl, 10 mM Tris-HCl, pH 7.5, 2.5 mM EDTA, 50% (v/v) ethanol], and DNA was removed from the beads by distilled water at 55 °C for 30 min.

DNA Purification from Agarose Gels by Electroelution and Filtration. After agarose gel electrophoresis for 1.5−2 h at 7 °C, the gel slice under the DNA band of interest was excised, and the resulting well was filled with electrophoresis buffer. Electrophoresis was continued for 2−3 min, DNA-containing buffer was removed from the well, and DNA was filtered on Ultrafree microcentrifuge filters (Sigma M-1161).

Radioactive Labeling. Polynucleotide kinase (Sibenzyme, 10 units/μL) and [γ-^{32}P]ATP (NEN; 3000 Ci/mmol, 10 mCi/mL) were used for 5′-labeling of the 1249 bp *p53* PCR product. The reaction was stopped by incubation at 65 °C during 15 min. The radiolabeled fragment was purified using a Sephadex G-50 column.

Extraction of Biotinylated DNA Duplexes. The DNA sample was added to an equal volume of streptavidin-coated magnetic particles (Dynabeads M-280 streptavidin) suspended in the 2× buffer: 10 mM Tris-HCl, pH 7.5, 1 mM EDTA, 2 M NaCl. It was incubated at room temperature using gentle rotation for 10 min. Then the pellet of beads coated with the biotinylated DNA fragment was washed two times with 1× buffer and once with PBS buffer diluted ten times by distilled H_2O. Then DNA was eluted by PBS buffer diluted ten times during 30 min at 60 °C.

Autoradiography. DNA was transferred to Hybond N+ nylon membrane from the agarose gel, and then the membrane was dried and exposed to Kodak film during 3 days at −70 °C.

Statistic Data Manipulation. The data obtained by gel processing using Scion Image 4.02 beta for Windows (http://www.scioncorp.com) from four parallel tracks of independent probes were taken for determination of the mean ± SD.

DNA Incubation Buffer. In all of the experiments DNA was incubated in 6 mM Tris-HCl, pH 7.5, 0.6 M NaCl, and 7 mM $MgCl_2$.

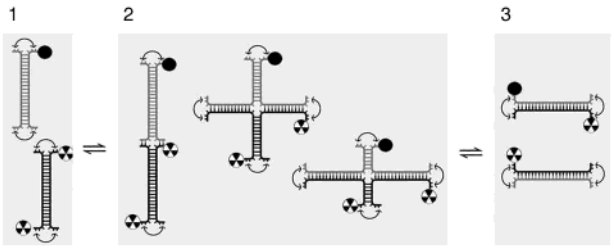

FIGURE 1: Strand exchange process in solution of homologous duplexes: (1) biotinylated and radiolabeled duplexes in nondenaturing conditions; (2) HJs formed by duplexes with different labels; (3) resolving of HJ with new duplex formation.

Electron Microscopy. DNA for electron microscopy was prepared using the protein monolayer technique (*26*). The specimens were investigated in a JEM 100CX electron microscope (JEOL, Japan) at 80 kV.

RESULTS

The Strand Exchange Process in a Solution of Linear Homologous Duplexes. To demonstrate the strand exchange process, we used two types of purified PCR products, which harbored absolute homology but differed by the labels. The biotin- and ^{32}P-labeled duplexes were used. After the duplexes are mixed, the process is proposed to proceed according to the scheme in Figure 1. Nonbiotinylated and biotinylated fragments were amplified and purified, and then nonlabeled ones were ^{32}P-labeled using polynucleotide kinase and [γ-^{32}P]ATP. The kinase reaction was stopped by 15 min incubation at 65 °C, which was observed to lead to complete loss of the polynucleotide kinase activity. Then the ^{32}P-labeled fragments were purified once again using Sephadex G-50. Biotinylated and radiolabeled fragment solutions (20 ng/μL) were mixed in equal parts at 4 °C, and the mixtures were incubated at 37 °C during 0 min, 1 h, 1 day, and 3 days. After incubation all samples were frozen, and before the consequent analysis every sample was divided into two equal parts. The first part of every sample was loaded on a gel directly. From the second part biotinylated fragments were extracted using streptavidin-coated magnetic particles. Using agarose gel electrophoresis we demonstrated that equal amounts of DNA were added into all of the mixtures (Figure 2A). Then the DNA was transferred to Hybond N+ nylon membrane. Using autoradiography we showed that portions of radiolabeled DNA fragments added to all of the mixtures were also equal (Figure 2B). Biotinylated fractions were extracted from the second parts of the mixtures and then were also loaded onto the gel. The electrophoretogram demonstrates that biotinylated fractions were successfully obtained and the amounts of biotinylated DNA were also equal in all samples (Figure 2C). DNA transfer to Hybond N+ nylon membrane followed by autoradiography revealed different levels of radioactivity of biotinylated fractions depending upon the incubation time (Figure 2D). The analysis of autoradiograms by the Scion Image program allowed us to determine the portion of biotinylated fraction radioactivity from the full mixture radioactivity (Figure 2E). Radioactivity of the biotinylated fraction extracted just after mixing was 1.00 ± 0.21% of the radioactivity of the corresponding mixture. This nonzero level of radioactivity is explained by a 15 min incubation of the mixture at 20 °C during the extraction of biotinylated duplexes. A 1 h

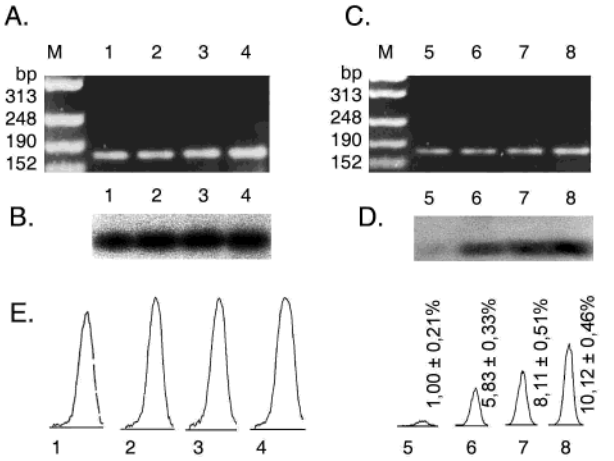

FIGURE 2: Increasing of radioactivity of biotinylated duplexes during their incubation in mixture with ^{32}P-labeled ones. M: molecular weight marker pBS+/*Hpa*I. Duration of incubation: lanes 1 and 5, 0 min; lanes 2 and 6, 1 h; lanes 3 and 7, 1 day; lanes 4 and 8, 3 days. Panels: (A) agarose gel electrophoresis demonstrating that equal amounts of DNA were taken into all mixtures; (B) radioactivity of the mixtures; (C) agarose gel electrophoresis demonstrating that equal amounts of biotinylated DNA were extracted from the mixtures; (D) radioactivity of biotinylated duplexes increasing dependently on duration of mixture incubation; (E) plots of the corresponding bands (B and D) obtained using the Scion Image program; a portion of the radioactivity of the biotinylated fraction was calculated as the ratio of pick squares correspondingly, 5 to 1, 6 to 2, 7 to 3, and 8 to 4, and indicated in percentage.

incubation of the mixture resulted in an increase of radioactivity in the biotinylated fraction up to 5.83 ± 0.33%. After a 1 day incubation it rose to 8.11 ± 0.51%. The maximum level of radioactivity in the biotinylated fraction was observed after a 3 day incubation, and it reached 10.12 ± 0.46%. Taking into consideration that only the antisense strand of the radioactive duplex may interact with the biotinylated sense strand, the level of the biotinylated fraction radioactivity could not exceed one-fourth of the radioactivity added to the mixture. According to our experimental estimation the efficiency of biotinylated fraction extraction using adsorption by streptavidin-coated magnetic particles followed by washing of DNA from the particles was about 50% in our performance. This means that the maximum level of radioactivity of the extracted biotinylated fraction may reach 12.5% of the radioactivity of the mixture. Correspondingly, the experimental value of radioactivity of the extracted biotinylated fraction after 3 day incubation was close to the maximum value calculated theoretically.

Influence of the Sequences of Duplex Ends on HJ Concentration. In previous analyses of homologous duplex solutions of 20 ng/μL or higher DNA concentration by gel electrophoresis, we have always revealed the band of HJs, but its intensity depended upon the conditions of purification and incubation (*3*). We have never observed a duplex solution of 20 ng/μL or higher DNA concentration without HJs formation during purification. Correspondingly, it was impossible to get a clear experimental kinetic dependence of HJ formation by linear duplexes. However, it was possible to compare equilibrium concentrations of HJs attained in different conditions. Previously, we demonstrated the dependence of the HJ equilibrium concentration on the fragment size, DNA concentration, and the incubation buffer composition.

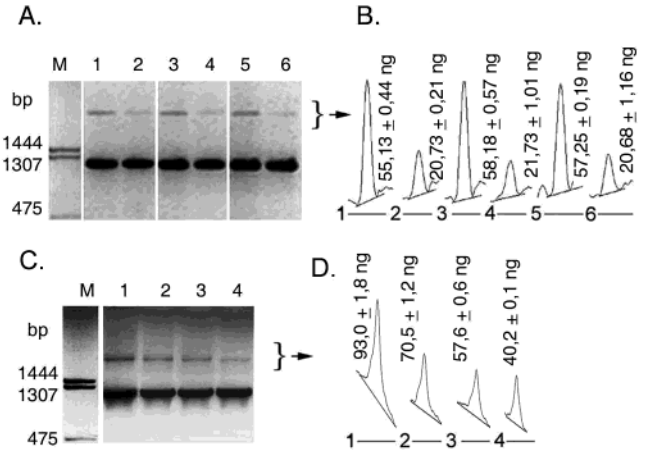

FIGURE 3: HJ yields in dependence on duplex end sequences: (A, C) electrophoresis of 20 μL of the fragment solutions (100 ng/μL); (B, D) plots corresponding to HJ bands determined by the Scion Image program and HJ yields calculated using calibration with pBR322/*Taq*I bands of known DNA amounts. (A, B) 1, 3, and 5, fragments with AT ends; 2, 4, and 6, fragments with GC ends; 1 and 2, 1 day; 3 and 4, 3 days; 5, 6, and 7 days; incubation was performed at 37 °C; M, pBR322/*Taq*I. (C, D) Incubation of the solutions of the fragments with AT ends at different temperatures: 1, at 10 °C; 2, at 25 °C; 3, at 37 °C; 4, at 55 °C.

To estimate the possible influence of the sequences of duplex ends on the equilibrium between HJs and duplexes, we used two 1254 bp fragments of human p53 cDNA differing only by their ends. One fragment was amplified using primers harboring at the 5′-end 7 base AT tails, and the other one was amplified using the same primers but with GC tails. The PCR products were purified, and their solutions were diluted until the equal concentration that was controlled by gel electrophoresis. For more accurate determination of duplex concentration we used several dilutions of the solution, and the intensity of the duplex bands were compared to the intensity of the bands of molecular weight marker pBR322/*Taq*I of known DNA amounts using the Scion Image program. Previously, we found that intensive HJ formation without significant appearance of additional more complex DNA structures occurred when the DNA concentration was 100 ng/μL (*3*). This DNA concentration was used as optimal for these experiments. To be sure that the equilibrium concentration of HJs was attained, we incubated solutions at 37 °C during 1, 3, and 7 days. After incubation samples were frozen to load them onto the gel simultaneously, and electrophoregrams were analyzed using the program "Scion Image" (Figure 3). There was no significant difference in HJ amounts after 1, 3, and 7 days of incubation. This means that the equilibrium between HJs and duplexes, characteristic for 37 °C, had been already attained after 1 day incubation. It was a clear difference between the intensity of HJ formation by the fragments harboring AT- and GC-rich end sequences (Figure 3A). Equilibrium concentrations of HJs were 2.84 ± 0.08 (4) ng/μL for the fragments with AT ends and 1.05 ± 0.03 (4) ng/μL for the fragments with GC ends (Figure 3B). Hence, after incubation of the solutions at 37 °C the intensity of the HJ band formed by the fragment with AT ends was 2.70 ± 0.06 (3) times more intensive comparatively to HJ band formed by the fragment flanked by GC sequences. We also analyzed the dependence of the equilibrium concentration of HJs on the temperature of incubation of DNA solutions (Figure 3C). Incubation of

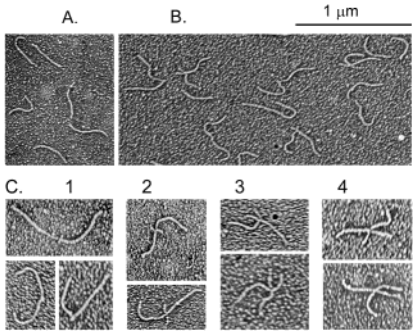

FIGURE 4: Electron microscopy of DNA structures: (A) in the fraction of ds fragments; (B) in the double size DNA fraction; (C) HJs with the cross point located within regions (1) 0−150 bp, (2) 150−300 bp, (3) 300−450 bp, and (4) 450−600 bp from the ends of the fragment.

solutions of the fragments with AT ends at 10 °C resulted in the increase of HJ concentration to 4.65 ± 0.09 ng/μL, while at 55 °C the concentration of HJ was 2.01 ± 0.05 ng/μL, lower than at 37 °C. The temperature effect on HJ concentration in solutions of the fragments with GC ends was opposite (results are not shown) but less intensive: at 10 °C the concentration of HJs was 1.2 times lower than at 37 °C, and it increased 1.15 times at 55 °C but it was still 1.4 times lower than HJ concentration in a solution of the fragments with AT ends at 55 °C.

Electron Microscopy of DNA Extracted from the Bands Analyzed. Previously, using electron microscopy we revealed four-way DNA structure formation in solutions of purified PCR product of cDNA of human p53 (*3*). Here we used the same DNA fragment but flanked by AT or GC sequences. Recently, Gaillard et al. revealed the formation of both four-stranded DNA (*4*, *5*) and hemicatenanes (*27*), which migrate slower than linear duplexes. Although the conditions of hemicatenane formation in their experiments differed from the conditions used in our work, electron microscopy analysis was performed to determine the DNA structure in all of the bands analyzed. DNA was extracted from the agarose gel via electroelution and was filtrated on microcentrifuged columns, and then the DNA solution was subjected to electron microscopy. Analysis of DNA fractions extracted from the bands of the ds PCR product harboring either AT or GC ends demonstrated predominantly linear fragments of the proper size, whereas many χ-structures were detected in the analysis of the DNA solution obtained from the bands of double size DNA structures. This occurred despite the fact that the concentrations of DNA used for the electron microscopy analyses were equal in all DNA solutions. The χ-structures observed could not be the result of overlapping as the concentration of DNA was low: the length of DNA structures was smaller than the distance between them, and the use of DNA solutions of lower concentration prepared directly before electron microscopy did not change the ratio between χ-structures and linear fragments. All four-stranded DNA structures observed were symmetrical, whereas the point of branch migration was located at different positions, and both *cis*- and *trans*-conformation structures were identified (Figure 4). The symmetry of all χ-structures observed also confirmed that it was not an overlapping. We analyzed the composition of HJ populations formed by the fragments with AT ends according to the location of the cross points. All HJs observed were separated into four groups according

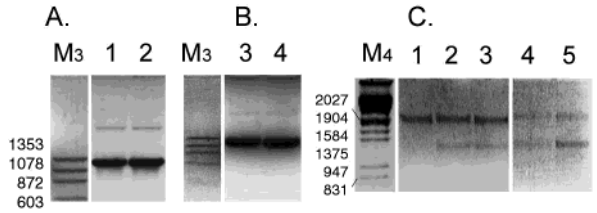

FIGURE 5: Influence of Triton X-100 on HJ formation and resolution. (A) HJ concentration in solutions of the fragments with AT ends: M_3, ϕX174/*Hae*III; M_4, λ/*Eco*RI, *Hin*dIII; (1) in the buffer containing 6 mM Tris-HCl, pH 7.5, 0.6 M NaCl, and 7 mM $MgCl_2$; (2) in the same buffer but with 1% of Triton X-100. (B) HJ concentration in solutions of the fragments with GC ends: (3) in the buffer containing 6 mM Tris-HCl, pH 7.5, 0.6 M NaCl, and 7 mM $MgCl_2$; (4) in the same buffer but with 1% of Triton X-100. (C) HJ resolving process. (1) HJ fraction just after purification. (2) Result of HJ incubation at 37 °C during 1 day in the buffer containing 6 mM Tris-HCl, pH 7.5, 0.6 M NaCl, and 7 mM $MgCl_2$. (3) Result of HJ incubation at 37 °C during 1 day in the buffer containing 6 mM Tris-HCl, pH 7.5, 0.6 M NaCl, 7 mM $MgCl_2$, and 1% of Triton X-100. (4) Result of HJ incubation at 37 °C during 3 days in the buffer containing 6 mM Tris-HCl, pH 7.5, 0.6 M NaCl, and 7 mM $MgCl_2$. (5) Result of HJ incubation at 37 °C during 3 days in the buffer containing 6 mM Tris-HCl, pH 7.5, 0.6 M NaCl, 7 mM $MgCl_2$, and 1% of Triton X-100.

to the position of the point of branch migration in the regions 0−150, 150−300, 300−450, and 450−600 bp from the ends of the fragments. The groups are represented in Figure 4C. Summarizing the results of electron microscopy analyses in which more than 700 HJs were observed, we can conclude that a great part of HJs, 0.76 ± 0.10 of the HJ population, belongs to the first group of HJs with the cross-point location at the 150 bp regions of the fragment ends, 0.18 ± 0.05 of the whole number of HJs harbored the cross point at the region 150−300 bp from the fragment ends, and the contribution of the third and fourth groups to the whole population was 0.04 ± 0.04 and 0.02 ± 0.01 correspondingly. Hence, the structures of DNA extracted from the bands of double size DNA complexes were HJs with the cross point located generally at the region of 300 bp of the fragment ends.

Independence of Holliday Junction Formation on Polypropylene Surfaces. The influence of polypropylene tube surfaces on DNA duplex denaturing was demonstrated in a number of previous investigations (*5*, *6*, *25*), and the mechanism of the DNA complex formation by interaction of denatured ss regions of DNA fragments was proposed to explain formation of multistranded DNA complexes by the fragments containing CA repeats (*6*). To analyze whether polypropylene surfaces influence HJ formation by homologous duplexes, we estimated the concentration of HJs after 3 day incubation in the presence or in the absence of Triton X-100. The Triton X-100 presence did not affect the intensity of HJ bands formed by the fragments with either AT or GC ends after a 3 day incubation at 37 °C (Figure 5). However, during the incubation of DNA extracted from the HJ band in both the presence and absence of Triton X-100, we observed HJ resolution into duplexes. This suggests that Triton X-100 does not stabilize HJ, and constant HJ concentration in solutions of homologous duplexes in the presence of Triton X-100 may be observed only if Triton X-100 does not have an influence on HJ formation.

Calculation of the Difference of the Free Energy for DNA Branching in Dependence on the Duplex End Sequences. Determination of the ratio between the HJ equilibrium concentrations affords us to calculate the free energy difference of the fragments with different end sequences for reacting two duplexes to give a four-arm junction. The free energy for the reaction of fragments with AT ends may be found as follows:

$$\Delta G^\circ_{AT} = -RT \ln K_{AT}$$

$$K_{AT} = C_{HJAT}/(C_{dsAT})^2$$

where K_{AT} is an equilibrium constant of the reaction of HJ formation by two duplexes with AT ends, C_{HJAT} is the concentration of HJ, and C_{dsAT} is the concentration of duplexes.

The free energy for the reaction of fragments with GC ends may be found as follows:

$$\Delta G^\circ_{GC} = -RT \ln K_{GC}$$

$$K_{GC} = C_{HJGC}/(C_{dsGC})^2$$

where K_{GC} is an equilibrium constant of the reaction of HJ formation by two duplexes with GC ends, C_{HJGC} is the concentration of HJ, and C_{dsGC} is the concentration of duplexes.

We may have found the difference: $\Delta G^\circ_{AT} - \Delta G^\circ_{GC} = -RT \ln(K_{AT}/K_{GC})$. As we used equal concentration, $C_{dsAT} = C_{dsGC}$, and as $C_{HJ} \ll C_{ds}$, we ignore the duplex portion spent for HJ formation:

$$\Delta G^\circ_{AT} - \Delta G^\circ_{GC} = -RT \ln(C_{HJAT}/C_{HJGC})$$

The ratio C_{HJAT}/C_{HJGC} was found to be 2.7 ± 0.06. Substituting numerical values of R, universal gas constant, temperature used, 310 K, and as 1 cal = 4.184 J, we found the difference in the free energy of the reactions:

$$\Delta G^\circ_{AT} - \Delta G^\circ_{GC} = -RT \ln 2.7 = -0.6 \text{ kcal/mol}$$

Thus, to form HJs, duplexes with AT ends require 0.6 kcal/mol less energy than homologous duplexes with GC ends.

DISCUSSION

The Spontaneous Strand Exchange Process in DNA Solutions. Strand exchange processes have been already demonstrated in mixtures of homologous DNA duplexes and ss fragments (*5*). If ss fragments were radiolabeled, their incubation in mixture with corresponding duplexes leads to appearance of radioactivity in ds fragments. The mechanism of the strand exchange process between homologous ss and ds DNAs was analyzed by Reynaldo et al. (*28*) using labeled oligonucleotides bound to a complementary DNA target and an unlabeled probe of the same sequence. The overall replacement rate was a combination of dissociative and sequential displacement pathways. The first one occurs by the spontaneous dissociation of the initial duplex followed by association of the target and unlabeled probe. The second one required only the partial melting of the initial duplex to allow for the formation of a branched nucleation complex, followed by the complete displacement of the labeled probe by migration of the branch point. At physiological conditions,

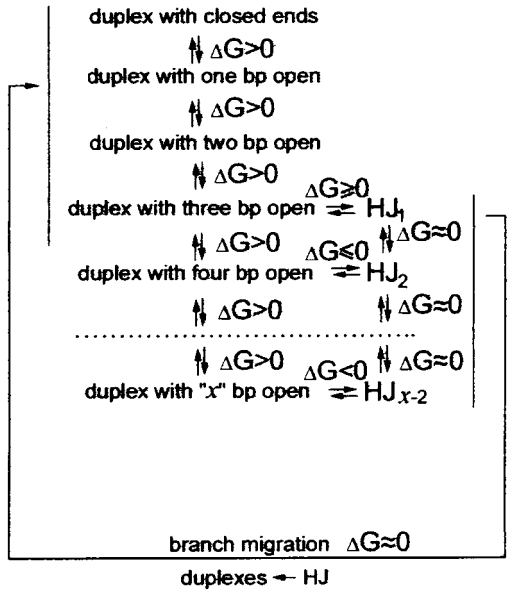

FIGURE 6: Kinetic consideration of the process of DNA duplex interaction via HJ formation.

the second mechanism, the sequential displacement, was predominant.

In the process of strand exchange between duplexes the radioactive strand moves up from one duplex to form another identical duplex. To reveal this process, we used two types of labeling. We used the biotin label as it allows easy extraction of biotinylated duplexes from DNA fragment mixtures. We have clearly demonstrated appearance of radioactivity in the biotinylated fraction. Polynucleotide kinase was completely inactivated after the kinase reaction, and then the labeled duplexes were purified thoroughly. The efficiency of purification was controlled by electrophoresis. Consequently, our results provide evidence of the strand exchange process between homologous duplexes. As we used nondenaturing conditions, and previously after DNA purification procedure we never observed the appearance of ss DNA by both gel electrophoresis and electron microscopy, this process is believed not to occur via dissociation−association. This issue is in accordance with data of Renaldo et al. (*28*) that the strand exchange process between ds and ss DNA at physiological conditions occurs by a sequential displacement mechanism. On the whole, the results of this experiment in combination with our previous electron microscopy data (*3*) show that in solutions of homologous duplexes the strand exchange process occurs via formation of HJs followed by branch migration resulting in the resolution into new or previously existing duplexes.

The Role of the Duplex Ends in DNA−DNA Interaction. According to our hypothesis, the spontaneous homologous duplex interaction is initiated by nucleation of the dissociated duplex ends (Figure 6). The nucleus formation is preceded by the several base pair opening at the duplex ends, which requires overcoming a large energy barrier. The more base pairs participating in nucleation, the more stable the HJs formed. However, the energetically unfavorable character of slowing down the end opening makes this process involve the small number of end base pairs as sterically possible for the HJ formation. The process of HJ formation may involve different numbers of end base pairs, and each pathway is characterized by its own probability. Further branch migration requires some time for back-resolution of HJ to duplexes. Thus, equilibrium concentration of HJs in duplex solution should depend on the duplex end dissociation, nucleation of complementary ends of two duplexes, and duration of branch migration process until complete resolution of HJ into duplexes. Recently, the free energy for dissociation and melting temperature of duplex end sets were estimated in the model of short oligonucleotide probes (*16*). It was shown that dissociation of AT-containing duplex ends requires much less energy comparatively to GC-containing ones. Therefore, we propose that sequences of duplex ends may influence the HJ equilibrium concentration. To determine the number of base pairs at the fragment ends sufficient for the influence on HJ equilibrium concentration, we considered the investigation of the nucleation process between ss complementary strands. Porschke showed that nucleation of the first three base pairs of two complementary ss DNAs is an unfavorable process, and only after involving the fourth base pair does the interaction become energywise favorable (*29*). Taking into consideration that, at the cross point of HJ, two or three base pairs are not bonded, we may conclude the necessity of 6−7 base pairs opening at the duplex ends to form HJ. Also, we considered the theoretical analysis of D-loop dissociation, in which the maximum number of base pairs involved in nucleation to form stable HJ was calculated to be 8 (*23*). It was impossible to estimate the duration of the full process in our system directly using the approach of Belotserkivskii and Zarling (*23*), as the final product of branch migration is the substrate of the reaction. However, if we take into account that in our system the process of nucleation is less favorable, we can conclude that the number of base pairs required to be open could not be less than in the process of D-loop dissociation. Therefore, 7−8 base pair tails of AT or GC sequences were added to 5′ ends of the primers.

Our analysis of the equilibrium HJ concentrations in solutions of duplexes flanked by either AT or GC sequences entirely confirmed the influence of the sequence of duplex ends on the interaction. As the process of branch migration is almost isoenergetic, the end sequences hardly influence HJ resolution into duplexes via branch migration, although the difference in energy of their opening is clear (*16*). Thus, end sequences may influence only the first steps of the process of duplex interaction. These data support our proposal that the process of HJ formation is initiated at duplex ends. This is in accordance with our electron microscopy analysis, in which we never revealed two cross points in any complex DNA structure formed by two PCR products; they should be observed in case of the interaction of internal regions of double-stranded DNA fragments. High frequency of the cross-point location at the 300 bp region of the fragment ends also suggests that HJ formation is initiated by nucleation of dissociated fragment ends. Roughly we have estimated the probability of branch migration in a Holliday junction forward or backward as $^1/_2$. To reach the *n*th position from the end, the cross point should pass *n* positions forward. Hence, the probability that the cross point in the HJ reaches the *n*th position should be calculated as a product probability of *n* single acts of moving the cross point forward, i.e., $(1/2)^{10}$. Thus, only $(1/2)^{10} = 1/1024 \approx 0.1\%$ of HJs starting branch migration would pass 10 steps.

However, four-way junction migration is accompanied by the synchronized rotation of all of the duplex regions involved into the process (*23*). It makes the probability of forward branch migration higher comparatively to the reverse process probability. Our electron microscopy analysis demonstrates the four-way DNA structures in accordance with the above-mentioned understanding of the branch migration process, and it suggests that HJ formation is initiated by the interaction of fragment ends.

Dependence of Free Energy for DNA Branching on the Sequences of Fragment Ends. HJ formation includes both unfavorable duplex end opening and further favorable nucleation, although with the loss of the energy of 2−3 base pairings at the cross point. If the HJ is formed by 6 bp at the ends of the duplexes, then the free energy for its formation would be near to the free energy for dissociation of three base pairs at the fourth, fifth, and sixth positions from the end. Doktycz et al. determined the free energy for dissociation of 3 base pair sets second from the ends in dependence on their sequence (*16*). According to these data the fragments used in our experiments should harbor the free energy for dissociation of second from the ends 3 base pair sets as follows: 1.21 kcal/mol (TAT/ATA), 1.82 kcal/mol (ATT/AAT), 5.15 kcal/mol (CGC/GCG), and 5.37 kcal/mol (GCC/CGG). The process of the HJ formation by the fragments with AT ends may involve opening of more base pairs than the HJ formation by the fragments with GC ends, which should decrease the dependence of the free energy for the interaction on fragment end sequences. The experimentally found difference between the free energy for branching of GC- and AT-ending fragments was about 0.6 kcal/mol. We explained this low value of the parameter by the fact that our calculations based on experimental measurements of HJ concentrations took into account HJ structures both with cross points at the fragment ends and at more internal regions, and the free energy of the last ones should not differ in dependence on the end sequences almost at all.

On the whole, we have demonstrated that the spontaneous DNA−DNA interaction between homologous linear duplexes occurs via nucleation of dissociated ends of complementary fragments with HJ formation, which are resolved via branch migration into new or previously existing duplexes. Our data are in accordance with modern theories of DNA structure, duplex melting, and branch migration. Besides this, it reveals a new peculiarity of DNA duplexes.

ACKNOWLEDGMENT

We thank B. P. Belotserkovskii for very useful theoretical discussions, valuable suggestions, and constant interest to our work. We are grateful to Z. Ronai and N. P. Kisseljova for theoretical and methodological help, to J. Babon for critical and valuable comments, and to P. M. Chumakov for kindly donating the set of plasmids with human *p53* cDNA.

REFERENCES

1. Lu, M., Guo, Q., Marky, L. A., Seeman, N. C., and Kallenbach, N. R. (1992) *J. Mol. Biol. 223*, 781−789.
2. Yakubovskaya, M. G., Neschastnova, A. A., Lipatova, Z. V., Popenko, V. I., and Belitsky, G. A. (1999) *Biochemistry (Moscow) 64*, 1310−1314.
3. Yakubovskaya, M. G., Neschastnova, A. A., Humphrey, K. E., Babon, J. J., Popenko, V. I., Smith, M. J., Lambrinakos, A., Lipatova, Z. V., Dobrovolskaia, M. A., Cappai, R., Masters, C. L., Belitsky, G. A., and Cotton, R. G. (2001) *Eur. J. Biochem. 268*, 7−14.
4. Gaillard, C., and Strauss, F. (1994) *Science 264*, 433−436.
5. Gaillard, C., Flavin, M., Woisard, A., and Strauss, F. (1999) *Biopolymers 50*, 679−689.
6. Belotserkovskii, B. P., and Johnston, B. H. (1997) *Anal. Biochem. 251*, 251−262.
7. Marky, L. A., Kallenbach, N. R., McDonough, K. A., Seeman, N. C., and Breslauer, K. J. (1987) *Biopolymers 26*, 1621−1634.
8. Holliday, R. (1964) *Genet. Res. 5*, 282−287.
9. Whithouse, H. L. K. (1982) *Genetic Recombination: Understanding the Mechanism*, Wiley, New York.
10. Postow, L., Ullsperger, C., Keller, R. W., Bustamante, C., Vologodskii, A. V., and Cozzarelli, N. R. (2001) *J. Biol. Chem. 276*, 2790−2796.
11. Wasserman, S. A., and Cozzarelli, N. R. (1986) *Science 232*, 951−960.
12. Cox, M. M., and Lehman, I. R. (1987) *Annu. Rev. Biochem. 56*, 229−254.
13. Saenger, W. (1984) *Principles of Nucleic Acid Structure*, Springer-Verlag, New York.
14. Breslauer, K. J., Frank, R., Blocker, H., and Marky, L. A. (1986) *Proc. Natl. Acad. Sci. U.S.A. 83*, 3746−3750.
15. Chalikian, T. V., Volker, J., Plum, G. E., and Breslauer, K. J. (1999) *Proc. Natl. Acad. Sci. U.S.A. 96*, 7853−7858.
16. Doktycz, M. J., Morris, M. D., Dormady, S. J., Beattie, K. L., and Jacobson, K. B. (1995) *J. Biol. Chem. 270*, 8439−8445.
17. Nonin, S., Leroy, J. L., and Gueron, M. (1995) *Biochemistry 34*, 10652−10659.
18. Leijon, M., and Graslund, A. (1992) *Nucleic Acids Res. 20*, 5339−5343.
19. Panyutin, I. G., and Hsieh, P. (1994) *Proc. Natl. Acad. Sci. U.S.A. 91*, 2021−2025.
20. Lilley, D. M. J. (1997) *Proc. Natl. Acad. Sci. U.S.A. 94*, 9513−9515.
21. Muck, S. M., Fee, R. S., Millar, D. P., and Chazin, W. J. (1997) *Proc. Natl. Acad. Sci. U.S.A. 94*, 9080−9084.
22. Duckett, D. R., Murchie, A. I., Diekmann, S., von Kitzing, E., Kemper, B., and Lilley, D. M. (1988) *Cell 55*, 79−89.
23. Belotserkovskii, B. P., and Zarling, D. A. (2000) *J. Biomol. Struct. Dyn. 17*, 1057−1075.
24. Belotserkovskii, B. P., Reddy, G., and Zarling, D. A. (1999) *Biochemistry 38*, 10785−10792.
25. Belotserkovskii, B. P., and Johnston, B. H. (1996) *Science 271*, 222−223.
26. Davis, R. W., and Hyman, R. W. (1971) *J. Mol. Biol. 62*, 287−301.
27. Gaillard C., and Strauss, F. (2000) *BMC Struct. Biol. 1*, 1−7.
28. Reynaldo, L. P., Vologodskii, A. V., Neri, B. P., and Lyamichev, V. I. (2000) *J. Mol. Biol. 297*, 511−520.
29. Porschke, D. (1977) *Mol. Biol. Biochem. Biophys. 24*, 191−218.

BI015959T